Annals of Operations Research
https://doi.org/10.1007/s10479-018-3012-y

S.I.: CLAIO 2016

Interior/exterior-point methods with inertia correction strategy for solving optimal reactive power flow problems with discrete variables

Marielena Fonseca Tófoli[1] · Edilaine Martins Soler[2] · Antonio Roberto Balbo[2] · Edméa Cássia Baptista[2] · Leonardo Nepomuceno[1]

Abstract
Interior/exterior-point methods have been widely used for solving Optimal Reactive Power Flow problems (ORPF). However, the utilization of such methods becomes difficult when transformer taps and/or capacitor/reactor banks are more rigorously represented in the problem formulation by means of discrete control variables. This work investigates the solution of the ORPF problem when transformer tap ratios are modeled as discrete variables. The solution method proposed handles discrete variables by means of sinusoidal penalty function, while the penalized problems are solved by an exterior-point method. An inertia correction strategy is proposed in order to assure that only local minima are obtained for the penalized problems. New search directions are also investigated that combine predictor and corrector directions. Numerical simulations are performed involving the IEEE 14, 30 and 57 bus systems. The results show the efficiency of the proposed inertia correction strategy and also reveals that the proposed exterior-point method outperforms traditional interior-point methods in terms of the number of iterations and computation times.

Keywords Optimal reactive power flow · Interior/exterior-point methods · Mixed discrete nonlinear programming

✉ Leonardo Nepomuceno
leo@feb.unesp.br

Marielena Fonseca Tófoli
tofoli.mf@gmail.com

Edilaine Martins Soler
edilaine@fc.unesp.br

Antonio Roberto Balbo
arbalbo@fc.unesp.br

Edméa Cássia Baptista
baptista@fc.unesp.br

[1] Departamento de Engenharia Elétrica, Faculdade de Engenharia, Universidade Estadual Paulista (Unesp), Bauru, Brazil

[2] Departamento de Matemática, Faculdade de Ciências, Universidade Estadual Paulista (Unesp), Bauru, Brazil

Published online: 22 August 2018

Nomenclature

Constants

g_{km}	Series conductance of branch km that connects buses k and m;
b_{km}	Series susceptance of branch km that connects buses k and m;
b_{km}^{sh}	Shunt susceptance of branch km that connects buses k and m;
b_{k}^{sh}	Shunt susceptance associated with a capacitor/reactor bank connected to bus k;
P_{G_k}	Active power generated at bus k;
P_{C_k}	Active power demanded at bus k
Q_{G_k}	Reactive power generated at bus k;
Q_{C_k}	Reactive power demanded at bus k;
$Q_{G_k}^{min}$	Minimum reactive power generated at bus k;
$Q_{G_k}^{max}$	Maximum reactive power generated at bus k;
V_{k}^{min}	Minimum voltage magnitude limit at bus k;
V_{k}^{max}	Maximum voltage magnitude limit at bus k.

Sets

L	Transmission lines of the system;
T	Power transformers of the system;
Γ_{km}	Discrete set for transformer tap ratios in branch km;
Λ	Branches (power transformers and transmission lines);
G	Buses with voltage magnitude control (generation and synchronous condenser buses);
G'	Buses with voltage magnitude control except the slack bus;
C	Load buses;
B	All system buses;
Ω_k	Buses belonging to the first neighborhood of bus k.

Variables and Functions

V_k	Voltage magnitude at bus k;
V_m	Voltage magnitude at bus m;
V	Vector of voltage magnitudes of all buses;
θ_k	Voltage angle at bus k;
θ_{km}	Difference in voltage angles at buses k and m;
θ	Vector of voltage angles of all buses;
t_{km}	Transformer tap ratio of branch km;
t	Vector of transformer tap ratios of all power transformer;
P_{km}	Active power flow in branch km;
Q_{km}	Reactive power flow in branch km;
Q_{k}^{sh}	Reactive power generated by the *shunt* capacitor/reactor bank connected to bus k.

1 Introduction

The Optimal Reactive Power Flow (ORPF) problem is concerned with the calculation of reactive control variables that minimizes a specific criteria associated with a power system, while ensuring its physical and operational limits. This problem has been solved by using various optimization approaches, which involve reduced-gradient methods (Carpentier 1962;

Dommel and Tinney 1968), Newton methods (Sasson et al. 1973; Sun et al. 1984), interior-point methods (Granville 1994; Wu et al. 1994), exterior-point methods (Pinheiro et al. 2015), among many others.

When transformer tap ratios and/or capacitor/reactor banks are represented in detail by means of discrete variables, the ORPF becomes a mixed-discrete nonlinear programming problem, here referred to as D-ORPF (Discrete ORPF) problem. The solution of the D-ORPF problem is complicated by the presence of discrete variables, which introduce additional combinatorial issues to the problem, whose solution may be hard to find by means of available optimization packages.Therefore, strategies for coping with discrete variables in the D-ORPF problem have been recently investigated.

Three main approaches have been used for solving the D-ORPF problems: i) meta-heuristic based methods, which generally work over a discrete set (set of possible values that a discrete variable can assume) by initially setting specific discrete values for the discrete variables, according to some heuristic rule, and subsequently solving for the resulting iterative nonlinear optimization problems. Particle swarm (AlRashidi and El-Hawary 2007), genetic algorithms (Bakirtzis et al. 2002) and hybrid methods (Yan et al. 2006) are some of the examples of algorithms of such approach used for solving the D-ORPF. ii) approaches that are based on a initial relaxation of the discrete set, by treating the discrete variables as continuous, and thereafter adopting additional constraints so that these variables are progressively taken to feasibility in the discrete set. Benders decomposition (Rabiee and Parniani 2013), progressively rounding techniques (Macfie et al. 2010; Platbrood et al. 2014), and hybrid methods, such as the one that integrates cutting-plane algorithms and interior-point methods (Liu et al. 2009) are some examples of this approach for solving the D-ORPF problem; iii) recent methods solve a relaxed version of the D-ORPF problem by handling the discrete variables as continuous, together with penalty functions that aim at penalizing infeasible discrete values (Lage 2013; Soler et al. 2013). When the penalty function is minimized together with the objective function, discrete variables tend to iteratively assume feasible discrete values in the optimal solution. This method is gaining recent attention because it can be easily implemented by means of commercial optimization solvers with good numerical results.

The solutions provided by the methods associated with the first approach may be sub-optimal, since meta-heuristic approaches generally do not account for optimality conditions. Another drawback of such approaches is the computation time, which may become extremely large for large-scale power systems. The methods associated with the second and third approaches seem more promising for solving real problems.

In this paper, we propose an optimization method based on the third approach for handling the discrete values associated with transformer tap ratios. In Soler et al. (2013), a sinusoidal penalty function was specifically proposed for the D-ORPF problem. The basic idea is to adjust a sinusoidal function so that its minimum values coincide with the values of the discrete set. A penalized optimization problem is defined by adding such penalty function to the objective function of the original problem and also relaxing the constraints associated with discrete variables. The iterative solutions of the penalized problems tend to become feasible in relation to the discrete set. This adjustment is easily performed when the discrete set is composed of equally spaced values, which is generally the case for the set of transformer tap ratios. The utilization of the sinusoidal penalty function for handling more general D-ORPF problems, that involves the representation of discrete values for susceptances associated with capacitor/reactor banks must be appropriately adapted, since the discrete set for such susceptances is generally composed by non-equally spaced values. This problem is not handled in this paper, and is left for future research.

The penalty function has been successfully used for handling discrete values of transformer tap ratios in Soler et al. (2013). However, its utilization introduces additional nonlinearities and also new maxima and minima to the D-ORPF problem. In this paper, we show that some solutions obtained for the penalized problems via solution of the KKT nonlinear equations may result in points of maximum of the penalty function, thus resulting in non-discrete values for some discrete variables. Therefore, robust nonlinear techniques are necessary so that maxima are avoided and only local minima are found. In this paper we investigate the computational performance of predictor-corrector primal-dual interior and exterior-point methods for solving the problem together with an inertia correction strategy that aims at escaping from local maxima and finding only local minima associated with the problem.

The main contributions of the paper are summarized as follows. (i) We propose a specific predictor-corrector primal-dual exterior-point method for solving the D-ORPF problem; (ii) We propose a technique to scape from local maxima and find only local minima associated with the problem, which is based on the inertia correction of the reduced Hessian matrix of the problem; (iii) We propose new search directions, based on the predictor and corrector directions, and evaluate them in the context of the D-ORPF problem; (iv) We compare the computation performance of proposed exterior-point method with the traditional interior-point method for solving the problem.

In Sect. 2 the D-ORPF problem is mathematically formulated, taking into account the representation of transformer tap ratios as discrete variables. The solution approach proposed for solving the problem is described in Sect. 3. The handling of discrete variables is described in Sect. 3.1 while the exterior-point method is detailed in Sect. 3.2. Numerical results are described in Sect. 4. Final conclusions are drawn in Sect. 5.

2 Optimal reactive power flow problem

The Optimal Reactive Power Flow (ORPF) problem bas been used as an important tool for both planning and operation of electrical power systems. The D-ORPF version of the problem involves the detailed representation of transformer tap ratios and/or capacitor/reactor banks by means of discrete variables. The D-ORPF problem is mathematically formulated as in (1). It is concerned with the minimization of active power losses in the transmission system (1a), while representing: active and reactive power balance equations (1b) and (1c), respectively; limits in the reactive power generation of voltage-controlled buses (1d); limits in voltage magnitudes (1e) and also constraints on the discrete values for transformer tap ratios (1f).

$$\begin{aligned}
\text{Min} \quad & P(V,t,\theta) && \text{(1a)}\\
\text{s.a:} \quad & \Delta P_k(V,t,\theta) = 0, \forall k \in G' \cup C && \text{(1b)}\\
& \Delta Q_k(V,t,\theta) = 0, \forall k \in C && \text{(1c)}\\
& Q_{G_k}^{min} \le Q_{G_k}(V,t,\theta) \le Q_{G_k}^{max}, \forall k \in G && \text{(1d)}\\
& V_k^{min} \le V_k \le V_k^{max}, \forall k \in B && \text{(1e)}\\
& t_{km} \in \Gamma_{km}, \forall (k,m) \in T, && \text{(1f)}
\end{aligned}$$

where constants, sets, variables and functions associated with the problem are defined in the Nomenclature section. We emphasize that the formulation of the D-ORPF given in (1) disregards the discrete nature of susceptances associated with capacitor/reactor banks, which is left as future research.

The D-ORPF problem may involve various objective functions, such as: total real power losses, variable and fixed reactive power costs, fuel costs, deviation of a given voltage schedule, voltage stability margin, or a combination of different objectives as a multi-objective model. In this paper, we use real power losses, which is mathematically described in (2):

$$P\left(V,t,\theta\right)=\sum_{(km)\in\Lambda}g_{km}\left(\left(\frac{V_k}{t_{km}}\right)^2+V_m^2\right)-\frac{2g_{km}}{t_{km}}V_kV_m\cos\theta_{km}. \tag{2}$$

Mathematical functions for active and reactive power balance equations (1b) and (1c) are described in equations (3)–(4), respectively:

$$\Delta P\left(V,t,\theta\right)=\sum_{m\in\Omega_k}P_{km}-P_{G_k}+P_{C_k} \tag{3}$$

$$\Delta Q(V,t,\theta)=\sum_{m\in\Omega_k}Q_{km}-Q_{G_k}+Q_{C_k}-Q_k^{sh}. \tag{4}$$

When k is associated with the bus where the transformer tap ratio is altered, expressions for active and reactive power flows P_{km} and Q_{km} in a power transformer located at branch km are described as in (5) and (6), respectively:

$$P_{km}=g_{km}\left(\frac{V_k}{t_{km}}\right)^2-\frac{V_kV_m}{t_{km}}g_{km}\cos\left(\theta_{km}\right)-\frac{V_kV_m}{t_{km}}b_{km}\sin\left(\theta_{km}\right) \tag{5}$$

$$Q_{km}=-\left(\frac{b_{km}}{t_{km}^2}+b_{km}^{sh}\right)V_k^2+\frac{V_kV_m}{t_{km}}b_{km}\cos\left(\theta_{km}\right)\frac{V_kV_m}{t_{km}}g_{km}\sin\left(\theta_{km}\right), \tag{6}$$

otherwise, the expressions for P_{km} and Q_{km} are as in(7) and (8), respectively:

$$P_{km}=g_{km}{V_k}^2-\frac{V_kV_m}{t_{km}}g_{km}\cos\left(\theta_{km}\right)-\frac{V_kV_m}{t_{km}}b_{km}\sin\left(\theta_{km}\right) \tag{7}$$

$$Q_{km}=-\left(b_{km}+b_{km}^{sh}\right)V_k^2+\frac{V_kV_m}{t_{km}}b_{km}\cos\left(\theta_{km}\right)-\frac{V_kV_m}{t_{km}}g_{km}\sin\left(\theta_{km}\right). \tag{8}$$

Expressions for the reactive power generation in voltage controlled buses are given as in (9):

$$Q_{G_k}\left(V,t,\theta\right)=\sum_{m\in\Omega_k}Q_{km}+Q_{C_k}-Q_k^{sh}, \tag{9}$$

where capacitor/reactor banks provide a reactive power injection given as in (10):

$$Q_k^{sh}=b_k^{sh}V_k^2. \tag{10}$$

In the D-ORPF problem formulated here, the shunt susceptance b_k^{sh} is considered fixed in (10). Therefore, the reactive power injections do not vary with the shunt susceptance, but only with voltage magnitude. In more representative models, the values of such susceptances are allowed to vary within a set of discrete values, which is not under consideration in the present model. The discrete sets are under analysis in this paper only in what concerns the representation of the transformer tap ratios, which generally have constant range of variation in their discrete sets, and therefore, are directly handled by the sinusoidal penalty function described in Soler et al. (2013), which is also adopted in this paper.

The discrete values of transformer tap ratios in (1f) introduce some additional complexities in the solution of the D-ORPF problem, and turns it into a mixed-discrete nonlinear optimization problem. The method proposed here for solving this problem is described in the next section.

3 Solution approach

The solution approach here proposed for solving the D-ORPF problem involves the reformulation of problem (1), by means of relaxing the discrete constraints, (i.e. enabling the discrete variables to assume continuous values), and also by adding new terms in the objective function which penalize infeasible discrete variables (those that do not belong to their respective discrete sets). The Relaxed Optimal Reactive Power Flow (R-ORPF) problem that results from this procedure is a nonlinear programming problem that presents multiple local minimizers, and is difficult to solve. In this paper we adopt an exterior-point method which is based on the classic Lagrangian function for handling equality constraints, and on the modified logarithmic barrier function (Polyak 1992, 2014) for handling inequality constraints. The sinusoidal penalty function approach is described in Sect. 3.1. The exterior-point method is detailed in Sect. 3.2.

3.1 Sinusoidal penalty function and penalty methods

The basic idea of the penalty approach proposed in this paper consists in relaxing the discrete constraints and also adding new terms in the objective function so as to penalize unfeasible discrete variables. To handle such discrete variables, the penalty function must have some good numerical properties, such as: (i) be smooth and differentiable in its domain; (ii) have their minima coinciding with the values fixed in the discrete set; (iii) have finite, preferably small, values in all its domain; (iv) do not present Runge's phenomenon (large oscillations in its values).

The sinusoidal function, which is discussed in this section has all such good numerical properties: it is smooth and differentiable in the domain of real numbers; it may be adjusted to match its minima with equally-spaced discrete values; it's values are no bigger than one, and it does not present the Runge's phenomenon. Therefore, this function may be used as the required penalty function.

To better understand how the sinusoidal penalty function is used in the method, consider the D-ORPF problem in (1). With the purpose of handling the discrete values for transformer tap ratios in (1f), we adopt the sinusoidal penalty function (11), such as described in Soler et al. (2013):

$$\Phi\left(\gamma, t_{km}\right) = \gamma\left[sin\left(\frac{t_{km}}{t_{km}^{\sup} - t_{km}^{\inf}}\pi + \alpha\right)\right]^2, \tag{11}$$

where γ is the penalty factor that determines the magnitude of function Φ; $t_{km}^{\sup}$ and $t_{km}^{\inf}$ are the upper and lower nearest discrete values of t_{km}, respectively; α is a constant defined such that $0 \leq \alpha \leq \pi$, function $\Phi\left(t_{km}\right)$ which is null only for values of t_{km} such that $t_{km} \in \Gamma_{km}$ (discrete set), and the mathematical constant $\pi = 3.1416$. From its definition, we verify that $\Phi\left(\gamma, t_{km}\right)$ assumes positive values only when t_{km} assumes non-discrete values. Therefore, the function $\Phi\left(\gamma, t_{km}\right)$ is of the form (12):

$$\Phi\left(\gamma, t_{km}\right) = \begin{cases} 0, & \text{if } t_{km} \in \Gamma_{km} \\ \delta > 0, & \text{otherwise.} \end{cases} \tag{12}$$

We define the Relaxed Optimal Reactive Power Flow (R-ORPF) problem as in (13) by adopting the procedure: (i) add the penalty function (12) to the objective function of the original D-ORPF problem (1); (ii) perform a relaxation on the constraints (1f), enabling the discrete variables to assume continuous values within a specified range (13f):

$$\text{Min} \quad P(V,t,\theta) + \Phi(\gamma, t_{km}) \tag{13a}$$

$$\text{s.a:} \quad \Delta P_k(V,t,\theta) = 0, \forall k \in G' \cup C \tag{13b}$$

$$\Delta Q_k(V,t,\theta) = 0, \forall k \in C \tag{13c}$$

$$Q_{G_k}^{min} \leq Q_{G_k}(V,t,\theta) \leq Q_{G_k}^{max}, \forall k \in G \tag{13d}$$

$$V_k^{min} \leq V_k \leq V_k^{max}, \forall k \in B \tag{13e}$$

$$t_{km}^{min} \leq t_{km} \leq t_{km}^{max}, \forall (k,m) \in T, \tag{13f}$$

where t_{km}^{min} and t_{km}^{max} are the lowest and the highest values for t_{km}, respectively, in the discrete set.

The procedure for solving the problem (1) by the penalty method is as described in Luenberger and Ye (2008): Let $\{\gamma_m\}, m = 1, 2...$ be a sequence such that for each m, we have $\gamma_{m+1} \geq \gamma_m$. Then, for each m solve iteratively the penalized problem (13), obtaining a solution $(V,t,\theta)_m$. By using the convergence properties of the penalty methods described in Luenberger and Ye (2008), we conclude that the sequence of points $\{(V,t,\theta)_m\}$ generated by the penalty method when $\gamma \to \infty$ is a solution to the original problem (assuming that each iterative problem has a solution).

The introduction of function $\Phi(\gamma, t_{km})$ in (13a) penalizes infeasible (non-discrete) transformer tap ratios, so that the optimal solution must have only feasible discrete values. To better understand the effects of the penalty function in the objective function, consider a simple objective function $f(x) = x^2$ and its sum with the penalty function $\Phi(x) = 0.01\left(sin\left(\frac{x}{0.2}\pi\right)\right)^2$, where the discrete values are equally spaced by 0.2. Note that the penalty function introduces various local minima and maxima, to the problem, making its solution process more complicated (Fig. 1). For coping with such problem, this paper proposes an inertia correction strategy which assures the calculation of local minima only, which is further described in Sect. 3.2.

Another important numerical issue is the iterative values of $\gamma_m, m = 1, 2....$ If we adopt large values for γ_0, the penalty terms may become higher than the original objective function. In this case, the problem does not minimize the original objective function, but the penalty terms only. On the other hand, if a small value is adopted for γ_0, the penalty terms may not be effective in enforcing discrete values to transformer tap ratios.

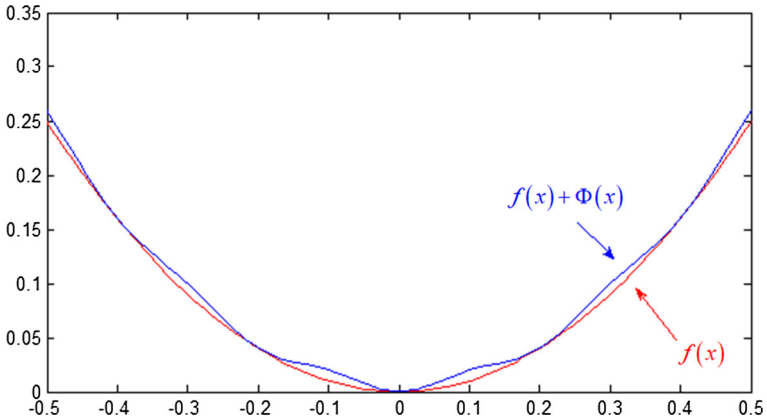

Fig. 1 Effect of the penalty function $\Phi(x) = 0.01\left(sin\left(\frac{x}{0.2}\pi\right)\right)^2$ in the objective function $f(x) = x^2$

The set of relaxed problems (13) correspond to difficult nonlinear problems to solve, due to inherent nonlinear formulation and also due to the nonlinearities introduced by the penalty function. The solution approach proposed for solving these problems is discussed in Sect. 3.2.

3.2 Exterior point method

In Soler et al. (2013) the set of Relaxed Optimal Reactive Power Flow (R-ORPF) problems (13) are solved by means of interior-point methods by using the computational package IPOPT (Wächter and Biegler 2005). In this work, we compare the computation performance of interior and exterior point methods for solving the R-ORPF problems.

In this section, the exterior point method is described with emphasis in the inertia correction strategy. For such a purpose, we put the problem (13) in the general form, as shown in (14):

$$\begin{aligned} &Min\ f(x) \\ &s.a \\ &\quad g(x) = 0 \\ &\quad h(x) \leq 0, \end{aligned} \tag{14}$$

where $x \in R^n$ and $f : R^n \rightarrow R$, $g : R^n \rightarrow R^m$ and $h : R^n \rightarrow R^p$ are of class C^2, with $n = 2 * |B| + |T|$, $m = |B| - 1 + |C|$ and $p = 2 * |\mathrm{G'}|$ for problem (13), where $|X|$ denotes the number of elements of set X.

With the purpose of applying the exterior-point method, inequality constraints are transformed into equivalent equalities by using slack variables $s \in R^p_+$ resulting in (15):

$$\begin{aligned} &Min\ f(x) \\ &s.a \\ &\quad g(x) = 0 \\ &\quad h(x) + s = 0 \\ &\quad s \geq 0. \end{aligned} \tag{15}$$

Non-negativity constraints are included in the modified problem (16) by means of a nonlinear rescaling function. Although in (16) the modified logarithmic barrier function is used, other rescaling functions could also be used:

$$\begin{aligned} &Min\ f(x) - \mu \sum_{i=1}^{p} \delta_i \ln\left(\mu^{-1} s_i + 1\right) \\ &s.a \\ &\quad g(x) = 0 \\ &\quad h(x) + s = 0, \end{aligned} \tag{16}$$

where $\mu > 0$ is the nonlinear rescaling parameter and $\delta \in R^p_+$ is the vector of Lagrange multiplier estimates associated with inequality constraints in (14). The classical Lagrangian function associated with the modified problem (16) is given in (17):

$$\begin{aligned} L_\mu(x, s, \lambda, \upsilon) = f(x) - \mu \sum_{i=1}^{p} \delta_i \ln\left(\mu^{-1} s_i + 1\right) \\ + \sum_{j=1}^{m} \lambda_j g_j(x) + \sum_{i=1}^{p} \upsilon_i [h_i(x) + s_i], \end{aligned} \tag{17}$$

where $\lambda \in R^m$ and $\upsilon \in R_+^p$ are the Lagrange multipliers associated with equality and inequality constraints in (14), respectively. One of the advantages of the modified logarithmic barrier function over the traditional logarithmic barrier function is that it is well defined in the boundary of the feasible set (Polyak 2014). This feature generally provides better computation times for this method over the traditional interior-point approach; It also provides the method with the ability to operate with points in the exterior of the feasible region.

3.2.1 System of directions

The exterior-point method consists in calculating a sequence of stationarity points for the Lagrangian function (17), which are obtained by solving the system of nonlinear equations given by $\nabla L_\mu(x, s, \lambda, \upsilon) = 0$. This system of equation is linearized in the neighborhood of $\left(x^k, s^k, \lambda^k, \upsilon^k\right)$ (associated with iteration k), resulting in the linear system show in (18):

$$\begin{bmatrix} K & 0 & Jg\left(x^k\right)^t & Jh\left(x^k\right)^t \\ 0 & \bar{S}_k^{-1} N^k & 0 & I_p \\ Jg\left(x^k\right) & 0 & 0 & 0 \\ Jh\left(x^k\right) & I_p & 0 & 0 \end{bmatrix} \begin{bmatrix} dx^k \\ ds^k \\ d\lambda^k \\ d\upsilon^k \end{bmatrix} = \begin{bmatrix} m^k \\ \bar{S}_k^{-1} r^k \\ t^k \\ u^k \end{bmatrix}, \tag{18}$$

where $K = \nabla^2_{xx} L\left(x^k, s^k, \lambda^k, \upsilon^k\right)$, I_p is the identity matrix of order p, $N^k = diag\left(\upsilon^k\right)$, $Jg\left(x^k\right)$, $Jh\left(x^k\right)$ are the Jacobian matrices associated with equality and inequality constraints, respectively, $\bar{S}_k^{-1} = diag\left(\frac{1}{s_1+\mu}, ..., \frac{1}{s_p+\mu}\right)$, and the residuals are calculated as in (19):

$$\begin{aligned} m^k &= -\nabla f\left(x^k\right) - Jg\left(x^k\right)^t \lambda^k - Jh\left(x^k\right)^t \upsilon^k \\ r^k &= -\bar{S}_k \upsilon^k + \mu\delta^k - ds^k \circ d\upsilon^k \\ t^k &= -g\left(x^k\right) \\ u^k &= -h\left(x^k\right) - s^k, \end{aligned} \tag{19}$$

where the nonlinear term $ds^k \circ d\upsilon^k$ denotes the Hadamard product (Horn and Johnson 1990).

The coefficient matrix in the left side of the system (18) is known as the Hessian of the Lagrangian function, which is rewritten in (20). This matrix plays a fundamental role in the solution of the linear system (18):

$$H^k = \begin{bmatrix} K & 0 & Jg\left(x^k\right)^t & Jh\left(x^k\right)^t \\ 0 & \bar{S}_k^{-1} N^k & 0 & I_p \\ Jg\left(x^k\right) & 0 & 0 & 0 \\ Jh\left(x^k\right) & I_p & 0 & 0 \end{bmatrix}. \tag{20}$$

As previously observed, the R-ORPF problem has multiple local minima and maxima, due to the sinusoidal penalty function used. Since the system of directions (18) is calculated using first order KKT conditions, which are valid for both maxima and minima, we may not assure that the solution of such direction system will lead to a desired local minima. In the next section, an inertia correction strategy is proposed so as to assure that only the desired minima are obtained.

3.2.2 Inertia correction strategy

As described in Silva (2014), the inertia of a matrix A is given by an ordered triplet $I(A) = (i_+, i_-, i_0)$, where i_+, i_-, i_0 are the numbers of positive, negative and null eigenvalues of matrix A, respectively (DApuzzo et al. 2010). According to Nocedal and Wright (2006), a descent direction is generated for the primal-dual system (18) if the sub-matrix A^k (upper diagonal of H^k) is positive-definite in the kernel of sub-matrix B^k associated with equality constraints, where

$$A^k = \begin{bmatrix} K & 0 \\ 0 & \bar{S}_k^{-1} N^k \end{bmatrix}; B^k = \begin{bmatrix} Jg\left(x^k\right) & 0 \\ Jh\left(x^k\right) & I_p \end{bmatrix}. \tag{21}$$

This condition occurs when the inertia of matrix H^k is given by $I(H^k) = (n+p, m+p, 0)$, where $n = 2 * |B| + |T|$, $m = |X| - 1 + |C|$ and $p = 2 * \left|G'\right|$.

In the predictor-corrector system of directions adopted in this paper, we work with a reduced version of system (18), by eliminating the directions ds^k and dv^k, to obtain an equivalent system of equations in terms of primal-dual directions dx^k and $d\lambda^k$, as given in (22):

$$\begin{bmatrix} \theta_k & Jg\left(x^k\right)^t \\ Jg\left(x^k\right) & 0 \end{bmatrix} \begin{bmatrix} dx^k \\ d\lambda^k \end{bmatrix} = \begin{bmatrix} m^k - p^k \\ t^k \end{bmatrix}, \tag{22}$$

where

$$\theta_k = K + Jh\left(x^k\right)^t \bar{S}_k^{-1} N^k Jh\left(x^k\right) \tag{23}$$

$$p^k = Jh\left(x^k\right)^t \bar{S}_k^{-1} \left(r^k - N^k u^k\right), \tag{24}$$

and the eliminated directions ds^k and dv^k are calculated using the values of direction dx^k and $d\lambda^k$ obtained from (22), according to (25) and (26), respectively:

$$ds^k = u^k - Jh\left(x^k\right) dx^k \tag{25}$$

$$dv^k = \bar{S}_k^{-1} \left(n^k - N^k ds^k\right). \tag{26}$$

In the reduced primal-dual system (22), a descent direction is generated if matrix $\hat{A}_k$ in the left side of (22) has an inertia $I(\hat{A}^k) = (n, m, 0)$, where

$$\hat{A}_k = \begin{bmatrix} \theta_k & Jg\left(x^k\right)^t \\ Jg\left(x^k\right) & 0 \end{bmatrix} \tag{27}$$

Computation of the inertia $I(\hat{A}^k)$ is performed in this paper by using LDL decomposition, where L is a lower triangular matrix and D is a diagonal matrix. Numerical issues and references regarding the calculation of matrix inertia are provided in DApuzzo et al. (2010). If matrix $\hat{A}_k$ does not have the appropriate inertia, alterations are necessary to correct it. The strategy adopted for correcting $I(\hat{A}_k)$ consists in adding terms to the diagonal of θ_k, which results in matrix $\tilde{A}_k$, as shown in (28):

$$\tilde{A}_k = \begin{bmatrix} \theta_k + \beta I_n & Jg\left(x^k\right)^t \\ Jg\left(x^k\right) & 0 \end{bmatrix} \tag{28}$$

Therefore, matrix $\tilde{A}_k$ replaces $\hat{A}_k$ in the left side of (22). The value of β that corrects $I(\tilde{A}_k)$ to the desired value is not known a priori. Therefore, successive higher values for β

are calculated using (29) until the matrix inertia reaches the appropriate value:

$$\beta_{k+1} = \kappa_1 \beta_k, \tag{29}$$

where $\kappa_1 > 1$ is a previously established parameter.

The importance of this inertia correction strategy in the solution of the R-ORPF problems is highlighted by means of simulation examples in the Results Section. In the following section, predictor and corrector steps are detailed.

3.2.3 Predictor and corrector steps

In the predictor step the nonlinear Hadamard product terms $ds^k \circ d\upsilon^k$ are neglected in the calculation of the residual expression r^k, as suggested in Mehrotra (1992). Therefore, the approximate value of r^k, given by $\tilde{r}^k$, is rewritten as $\tilde{r}^k = -\bar{S}_k \upsilon^k + \mu\delta^k$. Thereafter, the directions of the predictor step are calculated by using system (18), and exploiting sparsity of matrix H to isolate the direction terms, which are shown in (30):

$$\begin{aligned}
\tilde{d}\lambda^k &= \Theta_k^{-1}\left[Jg\left(x^k\right)\theta_k^{-1}\left(m^k - \tilde{p}^k\right) - t^k\right] \\
\tilde{d}x^k &= \theta_k^{-1}\left[m^k - \tilde{p}^k - Jg\left(x^k\right)^t \tilde{d}\lambda^k\right] \\
\tilde{d}s^k &= u^k - Jh\left(x^k\right)\tilde{d}x^k \\
\tilde{d}\upsilon^k &= \bar{S}_k^{-1}\left(\tilde{r}^k - N^k \tilde{d}s^k\right),
\end{aligned} \tag{30}$$

where

$$\begin{aligned}
\theta_k &= K + \beta I_n + Jh\left(x^k\right)^t \bar{S}_k^{-1} N^k Jh\left(x^k\right) \\
\Theta_k &= Jg\left(x^k\right)\theta_k^{-1} Jg\left(x^k\right)^t \\
\tilde{p}^k &= Jh\left(x^k\right)^t \bar{S}_k^{-1}\left(\tilde{r}^k - N^k u^k\right).
\end{aligned} \tag{31}$$

In the corrector step, the Hadamard terms are now calculated using the values obtained in the predictor step for $\tilde{d}s^k$ and $\tilde{d}\upsilon^k$. With an analogous procedure, we calculate the directions for the corrector step, which are shown in (32):

$$\begin{aligned}
d\lambda &= \Theta_k^{-1}\left[Jg\left(x^k\right)\theta_k^{-1}\left(m^k - p^k\right) - t^k\right] \\
dx^k &= \theta_k^{-1}\left[m^k - p^k - Jg\left(x^k\right)^t d\lambda^k\right] \\
ds^k &= u^k - Jh\left(x^k\right)dx^k \\
d\upsilon^k &= \bar{S}_k^{-1}\left(r^k - N^k ds^k\right),
\end{aligned} \tag{32}$$

where

$$p^k = Jh\left(x^k\right)^t \bar{S}_k^{-1}\left(r^k - N^k u^k\right). \tag{33}$$

In this paper, we investigate other possible search directions other than the predictor and corrector directions already defined. For such a purpose, we define the primal-dual point $\omega^k = \left[x^k, s^k, \lambda^k, \upsilon^k\right]^t$ as well as predictor and corrector directions, given by

$d\tilde{\omega}^k = \left[\tilde{\alpha}_k^P \tilde{d}x, \tilde{\alpha}_k^P \tilde{d}s, \tilde{\alpha}_k^D \tilde{d}\lambda, \tilde{\alpha}_k^D \tilde{d}\upsilon\right]^t$ and $d\omega^k = \left[\alpha_k^P dx, \alpha_k^P ds, \alpha_k^D d\lambda, \alpha_k^D d\upsilon\right]^t$, respectively. Based on these definitions we also define two auxiliary primal-dual points $\tilde{\omega}_k^I$ and ω_k^I, calculated as (34) and (35), respectively:

$$\tilde{\omega}_k^I = \omega_k + d\tilde{\omega}^k \tag{34}$$

$$\omega_k^I = \omega_k + d\omega^k \tag{35}$$

where $\tilde{\alpha}_k^P$ and $\tilde{\alpha}_k^D$ are primal and dual step lengths for the predictor step, respectively, while α_k^P and α_k^D are primal and dual step lengths for corrector step, respectively. The calculation of such steps is performed so as to assure that $\tilde{\omega}_k^I$ and ω_k^I are interior-points of the extended feasible region. In the exterior-point method the interior region is extended by the barrier parameter μ. Using the auxiliary points (34) and (35), we define new direction strategies in the next section.

3.2.4 Direction strategies, rescaling parameter update and stopping criteria

In most predictor-corrector approaches a search direction is calculated by means of a predictor step and then updated in the corrector step. However, we have experimentally verified that other search direction may even produce better numerical results (in some cases), such as, for instance, making a single predictor step (disregarding the corrector step), or even creating a direction that is a composition of the directions calculated in predictor and corrector steps.

The new strategies for calculating the directions in the method proposed are itemized below:

S1 The corrector directions $d\omega_k$ are used and the new solution point ω_{k+1} is given by ω_k^I in (35);

S2 We choose the most promising direction, by calculating the complementarity values $\tilde{\xi} = \left(\tilde{s}^k\right)^t \tilde{\lambda}^k$ and $\xi = \left(s^k\right)^t \lambda^k$ for predictor and corrector steps, respectively. The new solution point ω_{k+1} is given by $\tilde{\omega}_k^I$ in (34) if $\tilde{\xi} < \xi$, or by ω_k^I in (35), otherwise;

S3 We choose the direction proposed in Colombo and Gondzio (2007), which is a composition of predictor and corrector directions, where a new direction d_{S3} is chosen such that $d_{S3} = d\tilde{\omega}_k + \sigma d\omega_k$, with $\sigma > 0$. Next, primal and dual step lengths for the corrector step (α_k^P and α_k^D) are recalculated to assure that the new point will remain in the interior of the extended feasible region. Finally the new point ω_{k+1} is calculated as: $\omega_{k+1} = \omega_k + d_{S3}$;

S4 We choose a new direction d_{S4} which is a convex combination of predictor and corrector directions, such that $d_{S4} = \sigma_1 d\tilde{\omega}_k + \sigma_2 d\omega_k$. Next, primal and dual step lengths for the corrector step (α_k^P and α_k^D) are recalculated to assure that the new point will remain in the interior of the extended feasible region. Finally the new point ω_{k+1} is calculated as: $\omega_{k+1} = \omega_k + d_{S4}$.

The heuristic for updating the rescaling parameter μ, is based on a simple linear updating, using a fixed parameter. The Lagrange multipliers estimates are updated using the procedure described in Pinheiro et al. (2015), where the authors update the vector of Lagrange multiplier estimates δ^k in each iteration k by using the vector of dual variables υ^k associated with the inequality constraint of problem (14) at iteration k, as shown in (36):

$$\delta_i^k = \upsilon_i^k, i = 1, ..., p. \tag{36}$$

Stopping criterion involves a precision ϵ_1 over the infinity norm of the residuals given in (19).

4 Numerical results

In this section, the D-ORPF problem described in (1) is solved using the the proposed exterior point method described in Sect. 3.2 for the IEEE 14, 30 and 57 bus systems. Complete data for these systems are found in Chistie (2017). Results presented have three basic objectives: (i) evaluate the importance of the inertia correction strategy for obtaining feasible discrete solutions; (ii) compare the solutions obtained by the exterior point method proposed in this paper with those obtained by the traditional interior-point method, when the transformer tap ratios are represented as discrete variables by means of sinusoidal penalty functions described in Sect. 3.1 and (iii) evaluate the impact of the new direction strategies described in Sect. 3.2.4 for solving the D-ORPF problem in the exterior point method proposed.

In Sect. 4.1, the R-ORPF problem is solved considering transformer tap ratios as continuous variables, as described in (13). This solution is used as a reference to compare the results calculated for the cases where the D-ORPF problem (where discrete variables are represented in detail) is solved. Section 4.2 presents results that verifies the importance of the inertia correction strategy for obtaining feasible discrete solutions. In Sect. 4.3, the performance of interior and exterior point methods are compared for solving D-ORPF problems. The impact of the new search strategies for solving D-ORPF problems are evaluated in Sect. 4.4.

4.1 Solution of the relaxed ORPF

In this section, the R-ORPF problem is solved for all systems tested using the proposed exterior-point method. The main parameters used in the method are described in Table 1.

Tables 2, 3 and 4 show a synthesis of the solution obtained by interior (IPM) and exterior-point methods (EPM) for the R-ORPF problem. Values for the objective function, Lagrangian function, iteration number and the values calculated for transformer tap ratios for all systems are shown. The solutions obtained by both methods are identical for all systems. The calculated values for the Lagrangian and objective functions are also identical, a result that gives support to the good precision of the methods.

Table 1 List of parameter values used in the solution of the R-ORPF problem

Parameter	Description	Value
ϵ_1	Method precision	10^{-3}
ϵ_2	Precision for the discrete values	10^{-4}
μ	Initial value of the rescaling parameter	0.005
τ	Updating rate for μ	0.25
γ	Initial penalty value	10^{-5}
κ	Updating rate for γ	1.3
α	Phase value in the penalty function	0.0
β	Initial value for the inertia correction parameter	0.01
κ_1	Updating rate for β	1.5
V^{min}	Minimum value for voltage magnitudes	0.95
V^{max}	Maximum value for voltage magnitude	1.05
Γ_{km}	Set of discrete values for *taps*	{0.94, 0.96 0.98, 1.00, 1.02, 1.04}

Table 2 Solution of the R-ORPF problem for IEEE 14 bus system

IPM				EPM			
Obj. F.	Time	# it.	Tap	Obj. F.	Time	# it.	Tap
13.6415	0.28	5	$t_{5-6} = 1.0149$	13.6415	0.28	5	$t_{5-6} = 1.0149$
			$t_{4-7} = 0.9600$				$t_{4-7} = 0.9600$
			$t_{4-9} = 0.9916$				$t_{4-9} = 0.9916$

Table 3 Solution of the R-ORPF problem for IEEE 30 bus system

IPM				EPM			
Obj. F.	Time	# it.	Tap	Obj. F.	Time	# it.	Tap
17.8382	0.33	5	$t_{6-9} = 1.0344$	17.8382	0.31	5	$t_{6-9} = 1.0344$
			$t_{6-10} = 0.9600$				$t_{6-10} = 0.9600$
			$t_{4-12} = 1.0038$				$t_{4-12} = 1.0037$
			$t_{28-27} = 0.9600$				$t_{28-27} = 0.9605$

Table 4 Solution of the R-ORPF problem for IEEE 57 bus system

IPM				EPM			
Obj. F.	Time	# it.	Tap	Obj. F.		# it.	Tap
25.1867	0.41	6	$t_{4-18} = 0.9795$	25.1868	0.53	8	$t_{4-18} = 0.9793$
			$t_{4-18} = 0.9781$				$t_{4-18} = 0.9782$
			$t_{21-20} = 1.0027$				$t_{21-20} = 1.0027$
			$t_{24-25} = 0.9601$				$t_{24-25} = 0.9600$
			$t_{24-25} = 0.9601$				$t_{24-25} = 0.9600$
			$t_{24-26} = 0.9991$				$t_{24-26} = 0.9991$
			$t_{7-29} = 0.9731$				$t_{7-29} = 0.9731$
			$t_{34-32} = 0.9600$				$t_{34-32} = 0.9600$
			$t_{11-41} = 0.9600$				$t_{11-41} = 0.9600$
			$t_{15-45} = 0.9633$				$t_{15-45} = 0.9633$
			$t_{14-46} = 0.9601$				$t_{14-46} = 0.9600$
			$t_{10-51} = 0.9735$				$t_{10-51} = 0.9734$
			$t_{13-49} = 0.9599$				$t_{13-49} = 0.9599$
			$t_{11-43} = 0.9600$				$t_{11-43} = 0.9600$
			$t_{40-56} = 1.0142$				$t_{40-56} = 1.0142$
			$t_{39-57} = 0.9810$				$t_{39-57} = 0.9810$
			$t_{9-55} = 0.9668$				$t_{9-55} = 0.9667$

It is important to verify that some transformer tap ratios calculated do not belong to their respective discrete sets. Therefore a strategy for handling discrete variables is necessary to better represent such variables.

4.2 Proposed inertia correction strategy

In this section, we evaluate the proposed inertia correction strategy when penalty function methods are used to handle the discrete variables. For such a purpose, we compare the solutions obtained for the D-ORPF problems involving cases with and without the introduction of the proposed inertia strategy. The results are shown in Tables 5, 6 and 7 for the IEEE 14, 30 and 57 bus systems. These tables show the value of the objective function, the average number of iterations for performing the inertia correction (inner loop), the number of iterations, the value of transformer tap ratios, and the computation time for solving the systems.

Analyzing Table 5, we observe that the case where inertia correction is not taken into account presents infeasible discrete solutions for one transformer tap ratios. We observe that the lack of inertia correction strategy has a great impact on the methods trajectory, leading the method to points of maximum, instead of minima (associated with the penalty function). Note that the solution point $t_{4-7} = 0.9699$, for instance, is located in the intermediate point of the next lower and upper integer values (0.96 and 0.98), i.e. it is a point of maximum for the sinusoidal function. Although undesirable, this is an expected result, since both minima and maxima satisfies KKT optimality conditions. We observe that the solutions provided for the case with inertia correction strategy given in Table 5 are strictly feasible within the established precision for discrete variables. Observing the number of iteration in both cases we also verify the impact over the computation times regarding the penalty function method proposed to handle the discrete nature of the transformer tap ratios. Although the number of iterations for the case with inertia correction is substantially higher, the method proposed for handling the discrete variables does not have to solve a large number of cases, such as in the implicit enumerative methods, nor relies on heuristic procedures which do not assure local minima (KKT optimality conditions).

Table 5 Solution of the D-ORPF by the EPM method with and without inertia correction - IEEE 14 bus system

Case	Obj. F.	Inertia it.	#it.	Taps	Time
with	13,6685	4.33	9	$t_{5-6} = 0,9800$	0.26
				$t_{4-7} = 0.9600$	
				$t_{4-9} = 0.9600$	
without	13.7301	–	24	$t_{5-6} = 0,9800$	0.29
				$t_{4-7} = 0.9699$	
				$t_{4-9} = 0.9900$	

Table 6 Solution of the D-ORPF by the EPM method with and without inertia correction - IEEE 30 bus system

Case	Obj. F.	Iner. it.	#it.	Taps	Time
with	17.8933	26.76	18	$t_{6-9} = 1,0000$	1.19
				$t_{6-10} = 0.9800$	
				$t_{4-12} = 0.9800$	
				$t_{28-27} = 0.9799$	
without	18.0004	–	9	$t_{6-9} = 0,9800$	0.31
				$t_{6-10} = 0.9699$	
				$t_{4-12} = 1.0100$	
				$t_{28-27} = 0.9700$	

Table 7 Solution of the D-ORPF by the EPM method with and without inertia correction - IEEE 57 bus system

Case	Obj. F.	Iner. it.	#it.	Taps	Time
With	25.9188	19.46	40	$t_{4-18} = 1,0399$	12.98
				$t_{4-18} = 0.9999$	
				$t_{21-20} = 1.0399$	
				$t_{24-25} = 0.9600$	
				$t_{24-25} = 0.9600$	
				$t_{24-26} = 0.9999$	
				$t_{7-29} = 0.9799$	
				$t_{34-32} = 0.9599$	
				$t_{11-41} = 0.9599$	
				$t_{15-45} = 0.9600$	
				$t_{14-46} = 0.9600$	
				$t_{10-51} = 0.9600$	
				$t_{13-49} = 0.9600$	
				$t_{11-43} = 0.9600$	
				$t_{40-56} = 1.0000$	
				$t_{39-57} = 0.9799$	
				$t_{9-55} = 0.9600$	
Without	28.2518	–	75	$t_{4-18} = 0,9699$	2.01
				$t_{4-18} = 0.9800$	
				$t_{21-20} = 1.0399$	
				$t_{24-25} = 0.9799$	
				$t_{24-25} = 0.9999$	
				$t_{24-26} = 1.0500$	
				$t_{7-29} = 0.9699$	
				$t_{34-32} = 0.9599$	
				$t_{11-41} = 0.9599$	
				$t_{15-45} = 0.9600$	
				$t_{14-46} = 0.9700$	
				$t_{10-51} = 0.9599$	
				$t_{13-49} = 0.9500$	
				$t_{11-43} = 0.9700$	
				$t_{40-56} = 0.9600$	
				$t_{39-57} = 0.9800$	
				$t_{9-55} = 0.9600$	

Tables 6 and 7 show that similar conclusions can be obtained for systems with 30 and 57 buses. Note that for IEEE 30-bus system 3 taps are unfeasible in the solution for the case without the inertia correction strategy, while for IEEE 57-bus system, we identify 6 unfeasible taps.

From the results presented in this section, we conclude that the inertia correction strategy is necessary to assure local optimal solution of the D-ORPF problems.

4.3 Comparing exterior and interior-point methods

In this section the comparison between EPM and IPM for solving the D-ORPF problem is performed. The inertia correction strategy is adopted in all cases tested, since the results obtained in the last section pointed-out the need for such procedure both in IPM and EPM.

The computational implementation of the IPM used in this section has a structure that is similar to that of the EPM, where a primal-dual approach and a similar inertia correction are also used. The key difference between IPM and EPM lies in the way the sequence of points generated by the methods tends towards the boundary of the feasible region in the optimal solution. In the IPM method the sequence of points is within the interior of the feasible region, while in the EPM the sequence may generate points that come from external portions of the feasible region to its boundary. Generating an internal sequence of points is accomplished in the IPM by using the logarithmic barrier function $\ln(s_i)$ in (16) instead of the the modified logarithmic barrier function. Those functions are respectively used by the methods for handling inequality constraints in the slack variables of the problem (14). For such a purpose, some changes regarding the search directions provided in the EPM described in Sect. 3.2 are necessary to adapt it to run as an IPM method.

We have observed in the simulation results that the solutions of both methods depend on the initial value for the parameter κ_1 that updates the parameter β, which is associated with the inertia correction strategy. The results obtained for the methods are provided for $\kappa_1 = 1.3$. The comparison between the methods, for all systems tested, is shown in Tables 8, 9 and 10.

Analyzing Tables 8, 9 and 10, we observe that both EPM and IPM could find local optimal solutions for all systems tested (no unfeasibilitiy on discrete variables were found). Therefore,

Table 8 Comparison between EPM and IPM for solving the D-ORPF problem - IEEE 14 bus system

IPM				EPM			
Obj. F.	Time	# it.	Tap	Obj. F.	Time	# it.	Taps
$\kappa_1 = 1.30$							
13.6685	0.26	10	$t_{5-6} = 0.9800$	13.6685	0.26	9	$t_{5-6} = 0.9800$
			$t_{4-7} = 0.9600$				$t_{4-7} = 0.9600$
			$t_{4-9} = 0.9600$				$t_{4-9} = 0.9600$

Table 9 Comparison between EPM and IPM for solving the D-ORPF problem - IEEE 30 bus system

IPM				EPM			
Obj. F.	Time	# it.	Tap	Obj. F.	Time	# it.	Taps
$\kappa_1 = 1.30$							
17.8960	2.37	25	$t_{6-9} = 1.0399$	17.8982	1.35	18	$t_{6-9} = 0.9800$
			$t_{6-10} = 0.9600$				$t_{6-10} = 0.9600$
			$t_{4-12} = 0.9600$				$t_{4-12} = 0.9600$
			$t_{28-27} = 0.9600$				$t_{28-27} = 0.9600$

Table 10 Comparison between EPM and IPM for solving the D-ORPF problem - IEEE 57 bus system

IPM ($\beta_0 = 0.001$)				EPM ($\beta_0 = 0.01$)			
Obj. F.	Time	# it.	Tap	Obj. F.	Time	# it.	Taps
$\kappa_1 = 1.30$							
25.4607	12.26	41	$t_{4-18} = 0.9800$	25.6480	12.90	40	$t_{4-18} = 0.9800$
			$t_{4-18} = 0.9800$				$t_{4-18} = 0.9800$
			$t_{21-20} = 1.0399$				$t_{21-20} = 1.0399$
			$t_{24-25} = 0.9799$				$t_{24-25} = 0.9799$
			$t_{24-25} = 0.9799$				$t_{24-25} = 0.9799$
			$t_{24-26} = 1.0399$				$t_{24-26} = 1.0399$
			$t_{7-29} = 0.9600$				$t_{7-29} = 0.9600$
			$t_{34-32} = 0.9600$				$t_{34-32} = 0.9600$
			$t_{11-41} = 0.9600$				$t_{11-41} = 0.9600$
			$t_{15-45} = 0.9600$				$t_{15-45} = 0.9600$
			$t_{14-46} = 0.9600$				$t_{14-46} = 0.9600$
			$t_{10-51} = 0.9600$				$t_{10-51} = 1.0199$
			$t_{13-49} = 0.9600$				$t_{13-49} = 0.9600$
			$t_{11-43} = 0.9600$				$t_{11-43} = 0.9600$
			$t_{40-56} = 0.9600$				$t_{40-56} = 0.9800$
			$t_{39-57} = 0.9800$				$t_{39-57} = 0.9799$
			$t_{9-55} = 0.9600$				$t_{9-55} = 0.9999$

they were both capable of handling the discrete variables. We observe that different local minima may be obtained. We also observe that the exterior-point method proposed has shown some improvement in relation to the IPM regarding the average number of iterations. As the theory suggests (Polyak and Griva 2004), the EPM is more stable in the boundary of the feasible region and is able to obtaining solution points that are exactly over this boundary. On the other hand, the IPM is well defined only in the interior of the feasible region, and is not able to reaching the boundary exactly.

4.4 Impact of new search direction procedures

In this section, the new search directions S1–S4, described in Sect. 3.2.4 are evaluated for solving the D-ORPF problem for the systems tested. In all experiments carried-out in this section the inertia correction strategy is considered.

In order to set the vales for parameters σ, σ_1 and σ_2 in search directions S1–S4, a sensitivity analysis has been performed. For calculating the best value for σ, we have solved the D-ORPF problem using σ values that varies from 0.1 to 1.0 using fixed steps of 0.1. Then, we adopt the value of σ that provides the best result, i.e. the one with lower objective function value and the lower number of iterations. An analogous sensitivity analysis has been carried out for parameter σ_1, also adopting values from 0.1 to 1.0, and using steps of 0.1. Note that the value of σ_2 is automatically calculated when σ_1 is fixed.

For the IEEE 14 bus system, we adopted $\sigma = 0.1$, for direction strategy S3 and $\sigma_1 = 0.6$, $\sigma_2 = 0.4$ for search direction S4. Table 11 summarizes the performance of the search directions strategies for IEEE 14 bus system. We observe that S1 and S4 obtain the same number

Table 11 Solution for the IEEE 14 bus system for all search direction strategies investigated

Strategy	Loss (MW)	Time	# it.
S1	13.6988	0.25	9
S2	13.6685	0.34	23
S3	13.6685	0.34	24
S4	13.6988	0.28	9

Table 12 Solution for the IEEE 30 bus system for all search direction strategies investigated

Strategy	Loss (MW)	Time	# it.
S1	17.9289	1.30	18
S2	17.9289	0.84	16
S3	17.8813	1.60	45
S4	17.9289	1.82	23

Table 13 Solution for the IEEE 57 bus system for all search direction strategies investigated

Strategy	Loss (MW)	Time	# it.
S1	25.648	12.64	40
S2	–	–	–
S3	25.7019	11.28	61
S4	25.4616	20.12	60

of iterations with identical loss values. All strategies obtained feasible discrete solutions for the problem.

For the IEEE 30 bus system, we adopted $\sigma = 0.1$, for S3 and $\sigma_1 = 0.6$, $\sigma_2 = 0.4$ for S4. Table 12 summarizes the performance of the search directions strategies for IEEE 30 bus system. We observe that S2 presented the lowest number of iterations. However, S3 obtained the best loss values but at a higher computational cost.

For the IEEE 57 bus system, we adopted $\sigma = 0.3$, for S3 and $\sigma_1 = 0.4$, $\sigma_2 = 0.6$ for S4. Table 13 summarizes the performance of the search directions strategies for IEEE 14 bus system. We observe that S1 presented the lowest number of iterations. However, S3 obtained the best loss values but at a higher computational cost.

5 Conclusions

This paper investigates some solution approaches to the Discrete Optimal Reactive Power Flow (D-ORPF) problem, which is formulated as a mixed-discrete nonlinear programming problem. The discrete nature of the problem is handled by sinusoidal penalty functions while the resulting nonlinear programming problem is solved using the proposed predictor-corrector primal-dual exterior-point method. An inertia correction strategy is also proposed, together with the exterior-point method, in order to avoid local maxima and provide a necessary global convergence strategy for finding only local minima. The proposed method, as well as a traditional interior-point method, are applied for solving the D-ORPF problem regarding the systems IEEE 14, 30 and 57 buses. The results show that the inertia correction strategy proposed is a fundamental tool for finding feasible solutions for the discrete variables. In other

words, the results show that if sinusoidal penalty methods are used for handling discrete variables, an inertia correction strategy must be used. The comparison of exterior versus interior-point methods shows advantage for the proposed exterior approach, in terms of the number of iterations and computational effort for solving the problem. However, both methods were able to finding optimal feasible solutions in terms of the discrete sets for all systems tested. We also propose four new search directions in the predictor-corrector primal-dual EPM method, which are basically a composition of the directions calculated in the predictor and corrector steps (as described in Sect. 3.2.4). The results involving these new search directions have been evaluated by analyzing the value of the objective function obtained in the optimal solution, as well as the number of iterations obtained by each direction strategy used. The results show that the direction adopted in the traditional predictor-corrector approach (which corresponds to S1) may not always be the best search direction to adopt; other directions may also successfully be adopted that provide lower objective function values and/or a reduced number of iterations.

Acknowledgements The authors would like to thank the anonymous reviewers for their relevant comments and questions that helped enhancing the paper significantly. We would like to thank Fundação de Amparo à Pesquisa do Estado de São Paulo—FAPESP (process numbers 2013/03388-0 and 2014/20853-0), Coordenação de Aperfeiçoamento de Pessoal de Nível Superior—CAPES and Brazilian National Research Council—CNPq (process numbers 309780/2017-9, 428740/2016-2 and 313495/2017-3).

References

AlRashidi, M. R., & El-Hawary, M. E. (2007). Hybrid particle swarm optimization approach for solving the discrete OPF problem considering the valve loading effects. *IEEE Transactions on Power Systems*, *22*(4), 2030–2038. https://doi.org/10.1109/TPWRS.2007.907375.

Bakirtzis, A. G., Biskas, P. N., Zoumas, C. E., & Petridis, V. (2002). Optimal power flow by enhanced genetic algorithm. *IEEE Transactions on Power Systems*, *17*(2), 229–236. https://doi.org/10.1109/TPWRS.2002.1007886.

Carpentier, J. (1962). Contribution a l'étude du dispatching economique. *Bulletin de la Société Française des Électricien*, *3*(8), 431–447.

Chistie, R. D. (2017). Power systems test case archive - UWEE. http://www2.ee.washington.edu/research/pstca/

Colombo, M., & Gondzio, J. (2007). Further development of multiple centrality correctors for interior point methods. *Computational Optimization and Applications*, *41*(3), 277–305. https://doi.org/10.1007/s10589-007-9106-0.

DApuzzo, M., Simone, V. D., & Serafino, D. D. (2010). On mutual impact of numerical linear algebra and large-scale optimization with focus on interior point methods. *Computational Optimization and Applications45*(2), 283–310. https://doi.org/10.1007/s10589-008-9226-1. https://link.springer.com/article/10.1007/s10589-008-9226-1

Dommel, H., & Tinney, W. (1968). Optimal Power Flow Solutions. *IEEE Transactions on Power Apparatus and SystemsPAS-87*(10), 1866–1876. https://doi.org/10.1109/TPAS.1968.292150

Granville, S. (1994). Optimal reactive dispatch through interior point methods. *IEEE Transactions on Power Systems*, *9*(1), 136–146. https://doi.org/10.1109/59.317548.

Horn, Roger A., & Johnson, C. R. (1990). *Matrix analysis*. Cambridge: Cambridge University Press.

Lage, G. G. (2013). O fluxo de potência ótimo reativo com variáveis de controle discretas e restrições de atuação de dispositivos de controle de tensão (in Portuguese). Ph.D. Thesis, Universidade de São Paulo - USP, São Carlos - SP

Liu, L., Wang, X., Ding, X., & Chen, H. (2009). A robust approach to optimal power flow with discrete variables. *IEEE Transactions on Power Systems*, *24*(3), 1182–1190. https://doi.org/10.1109/TPWRS.2009.2023258.

Luenberger, D. G., & Ye, Y. (2008). *Linear and nonlinear programming* (3rd ed.). New York, NY: Springer.

Macfie, P. J., Taylor, G. A., Irving, M. R., Hurlock, P., & Wan, H. B. (2010). Proposed shunt rounding technique for large-scale security constrained loss minimization. *IEEE Transactions on Power Systems*, *25*(3), 1478–1485. https://doi.org/10.1109/TPWRS.2010.2041675.

Mehrotra, S. (1992). On the implementation of a primal-dual interior point method. *SIAM Journal on Optimization*, *2*(4), 575–601. https://doi.org/10.1137/0802028.

Nocedal, J., & Wright, S. J. (2006). *Numerical optimization*., Springer series in operations research and financial engineering. New York, NY: Springer.

Pinheiro, R. B. N., Balbo, A. R., Baptista, E. C., & Nepomuceno, L. (2015). Interior-exterior point method with global convergence strategy for solving the reactive optimal power flow problem. *International Journal of Electrical Power & Energy Systems*, *66*, 235–246. https://doi.org/10.1016/j.ijepes.2014.10.003.

Platbrood, L., Capitanescu, F., Merckx, C., Crisciu, H., & Wehenkel, L. (2014). A generic approach for solving nonlinear-discrete security-constrained optimal power flow problems in large-scale systems. *IEEE Transactions on Power Systems*, *29*(3), 1194–1203. https://doi.org/10.1109/TPWRS.2013.2289990.

Polyak, R. (1992). Modified barrier functions (theory and methods). *Mathematical programming54*(1-3), 177–222. http://link.springer.com/article/10.1007/BF01586050

Polyak, R. (2014). Lagrangian Transformation and interior ellipsoid methods in convex optimization. *Journal of Optimization Theory and Applications*, *164*(3), 966–992. https://doi.org/10.1007/s10957-014-0527-5. http://link.springer.com/article/10.1007/s10957-014-0527-5.

Polyak, R., & Griva, I. (2004). Primal-dual nonlinear rescaling method for convex optimization. *Journal of Optimization Theory and Applications*, *122*(1), 111–156. https://doi.org/10.1023/B:JOTA.0000041733.24606.99.

Rabiee, A., & Parniani, M. (2013). Voltage security constrained multi-period optimal reactive power flow using benders and optimality condition decompositions. *IEEE Transactions on Power Systems*, *28*(2), 696–708. https://doi.org/10.1109/TPWRS.2012.2211085.

Sasson, A. M., Viloria, F., & Aboytes, F. (1973). Optimal load flow solution using the Hessian matrix. *IEEE Transactions on Power Apparatus and Systems PAS-92*(1), 31–41. https://doi.org/10.1109/TPAS.1973.293590

Silva, D. N. (2014). Método primal-dual previsor-corretor de pontos interiores e exteriores com estratégias de correção de inércia e suavização hiperbólica aplicado ao problema de despacho econômico com ponto de carregamento de válvula e representação da transmissão (in Portuguese). M.Sc. dissertation, Universidade Estadual Paulista "Júlio de Mesquita Filho", UNESP, Bauru - SP

Soler, E., Asada, E., & da Costa, G. (2013). Penalty-based nonlinear solver for optimal reactive power dispatch with discrete controls. *IEEE Transactions on Power Systems*, *28*(3), 2174–2182. https://doi.org/10.1109/TPWRS.2013.2252207.

Sun, D., Ashley, B., Brewer, B., Hughes, A., & Tinney, W.F. (1984). Optimal power flow by newton approach. IEEE Transactions on Power Apparatus and Systems *PAS-103*(10), 2864–2880. https://doi.org/10.1109/TPAS.1984.318284

Wächter, A., & Biegler, L. T. (2005). On the implementation of an interior-point filter line-search algorithm for large-scale nonlinear programming. *Mathematical Programming*, *106*(1), 25–57. https://doi.org/10.1007/s10107-004-0559-y.

Wu, Y. C., Debs, A., & Marsten, R. (1994). A direct nonlinear predictor-corrector primal-dual interior point algorithm for optimal power flows. *IEEE Transactions on Power Systems*, *9*(2), 876–883. https://doi.org/10.1109/59.317660.

Yan, W., Liu, F., Chung, C. Y., & Wong, K. P. (2006). A hybrid genetic algorithm-interior point method for optimal reactive power flow. *IEEE Transactions on Power Systems*, *21*(3), 1163–1169. https://doi.org/10.1109/TPWRS.2006.879262.